Supporting Information

On the application of consistency criteria to calculate BET areas of micro- and mesoporous metal-organic frameworks

Diego A. Gómez-Gualdrón [a‡], *Peyman Z. Moghadam* [a‡], *Joseph T. Hupp*[b], *Omar K. Farha*[b], *Randall Q. Snurr* [a]*

[a] Department of Chemical and Biological Engineering, Northwestern University, 2145 Sheridan Road, Evanston, IL 60208, USA

[b] Department of Chemistry and International Institute for Nanotechnology, Northwestern University, 2145 Sheridan Road, Evanston, Illinois 60208, USA

[c] Department of Chemistry, Faculty of Science, King Abdulaziz University, Jeddah, Saudi Arabia

* Corresponding author: snurr@northwestern.edu

TABLE OF CONTENTS

Section 1: Detailed computational methods

Nitrogen adsorption simulations

Calculated nitrogen adsorption isotherms at 77 K were obtained via grand canonical Monte Carlo (GCMC) simulations using our in-house RASPA code.[1] We used a minimum of 20,000 cycles for equilibration and an additional 20,000 cycles for data collection. In a cycle, *N* Monte Carlo steps are performed, where *N* is the maximum of 20 and the number of adsorbate molecules in the simulation supercell. All simulations included equal-probability insertion, deletion, rotation, and translation moves. The atoms of the adsorbent materials were maintained fixed during simulation. The interaction energies between atoms were calculated using the LJ plus Coulomb potential:

$$\mathcal{V}_{ij} = 4\varepsilon_{ij}\left[\left(\frac{\sigma_{ij}}{r_{ij}}\right)^{12} - \left(\frac{\sigma_{ij}}{r_{ij}}\right)^{6}\right] + \frac{q_i q_j}{4\varepsilon_0 r_{ij}}$$

where i and j are interacting atoms, r_{ij} is their interatomic distance, q_i and q_j are their Coulomb electrostatic charges, ε_{ij} is their LJ potential well depth, σ_{ij} is the distance at which repulsion between i and j occurs, and ε_0 is the dielectric constant. The ε_{ij} and σ_{ij} LJ parameters were obtained by applying the Lorentz-Berthelot mixing rules[2] to the LJ parameters of atoms i (σ_{ii} and ε_{ii}) and j (σ_{jj} and ε_{jj}). The LJ parameters for adsorbent atoms were obtained from the Universal Force Field (UFF)[3] as tabulated in **Table S1.1**.

Table S1.1. UFF LJ parameters used for adsorbent atoms

Atom type	σ (Å)	ε/k_B (K)
C	3.431	52.882
Co	2.559	7.045
Cu	3.114	2.516
O	3.118	30.218
H	2.571	22.160
N	3.266	34.571
Zn	2.461	62.399
Zr	2.783	34.751

The LJ parameters and electrostatic charges for the adsorbate atoms were obtained from the TraPPE force field[4] as schematized in **Figure S1.1**.

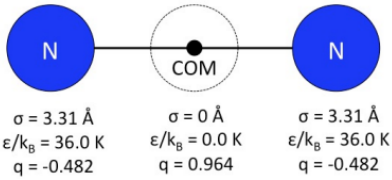

Figure S1.1. Electrostatic charges and LJ parameters for nitrogen molecules according to the TraPPE force field. This force field was fitted to reproduce the vapor-liquid coexistence of nitrogen. Nitrogen molecules are modeled as a three-site rigid model (N-N = 1.10 Å) that reproduces the experimentally determined quadrupole moment of nitrogen molecules.

The LJ potential was truncated at 12.8 Å (with no tail-corrections considered), and all simulations used the minimum *n* x *m* x *l* supercell needed to prevent atoms from interacting with their periodic images. The

Ewald summation method was used for the Coulomb interactions between adsorbate molecules. No Coulomb interactions between nitrogen molecules and framework atoms were considered, as Bae *et al.*[5] previously showed that this simplification has a negligible effect on simulated nitrogen isotherms at 77 K.

Pore size distribution calculations

Using the "σ" LJ parameter obtained from the Universal Force Field (UFF) to characterize the size of adsorbent atoms, the pore size distributions (PSDs) of the studied materials were calculated using the method of Gelb and Gubbins.[6] In this method, a large number of random points in the porous region of the materials are selected, and the diameter of the largest sphere that can enclose each point without contacting the pore walls is determined to generate a PSD histogram.

Analysis of simulation "snapshots"

***Nitrogen molecules contacting adsorbent atoms*:** We analyzed the "snapshots" obtained from the nitrogen simulations to obtain values such as the number of nitrogen molecules contacting adsorbent atoms or to determine the number of nitrogen molecules in different cage types. We did this using a python script that implements our analysis algorithms as follows. To determine whether a nitrogen molecules was contacting the adsorbent atoms or not, we define

$$\delta_{ij} = d_{ij} - 2^{1/6}\,\sigma_{ij}$$

where d_{ij} is the shortest center-to-center distance between any of the i atoms of the nitrogen molecule and any of the j atoms of the adsorbent material, and σ_{ij} is the LJ σ parameter for the corresponding pair of atoms involved. Thus, implementing a tolerance, the number of molecules that satisfies $\delta_{ij} < 1.0$ Å is defined as the number of molecules "contacting" the pore walls.

The rationale for using this tolerance is illustrated in **Figure S1.2. Figure S1.2-a** shows the LJ potential curve for the interaction of an adsorbent carbon atom and an adsorbate nitrogen atom. Ideally, in every simulation snapshot, adsorbed N_2 molecules contributing to the monolayer are located with all relevant N atom centers exactly at the equilibrium distance, as depicted in **Figure S1.2-b-**(left),. However, in reality, in a given simulation snapshot, adsorbed N_2 molecules contributing to the monolayer can appear with the relevant N atom centers slightly closer or farther than the equilibrium distance as depicted in **Figure S1.2-b-**(middle and right). Therefore, to count correctly how many molecules contribute to the monolayer, a tolerance is needed. Notice that with the used tolerance ($\delta_{ij} < 1.0$ Å), the relevant N center is still within the well depth according to **Figure S1.2-a**. The used tolerance was also validated by showing that it correctly captures the formation of the monolayer in graphene systems (see **Figure 2-a,c,e** in the main text).

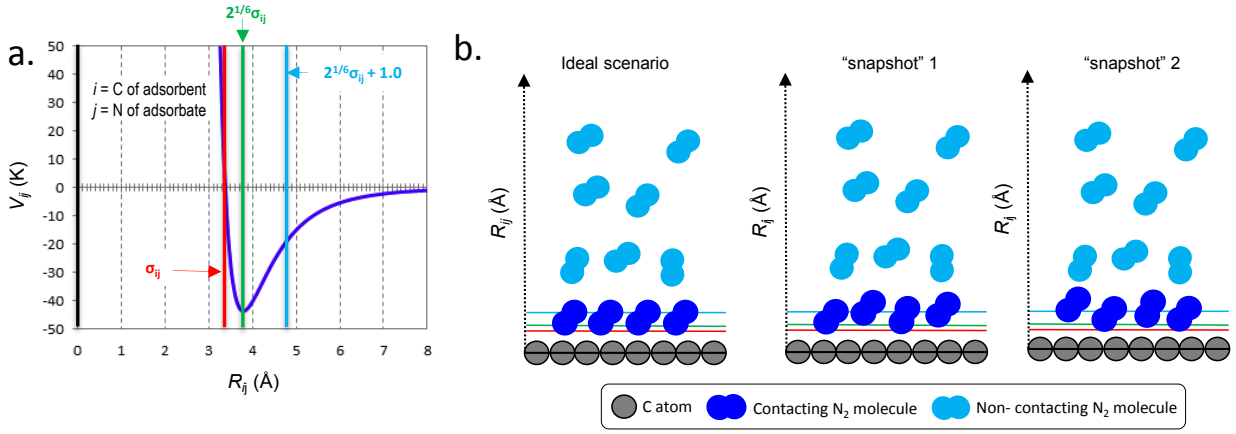

Figure S1.2. (a) LJ potential corresponding to the interaction between a carbon atom (of the adsorbent) and a nitrogen atom (of the adsorbate). At the equilibrium position the center-to-center distance between carbon and nitrogen is $2^{1/6}\sigma_{ij}$. (b) Schematics of simulation snapshots in graphene. The depicted sizes of N and C atoms (blue and gray, respectively) are equal to σ_{ij}. The positions of the black, red, green and blue horizontal lines correspond to the positions of the black, red, green and blue vertical lines in panel *a*. In an *ideal scenario*, "contacting" N_2 molecules (i.e. those that contribute to forming the N_2 adsorption monolayer) would appear in simulation snapshots as depicted in the *left schematic*: with the all N atom centers perfectly placed at the $2^{1/6}\sigma_{ij}$ (green line). However, contacting N_2 molecules in simulation snapshots appear as depicted in the *middle* and *right schematics* due to thermal motion.

***Classification of nitrogen molecules by MOF cages*:** To determine in which cage type a nitrogen molecule was located, the shortest center-to-center distances between any of the *i* atoms of the nitrogen molecule and strategically placed "cage marker points" were collected. By defining a distance criterion based on the cage dimensions particular to each material, each nitrogen molecule was uniquely assigned to a given cage type.

Nitrogen-accessible surface area (NASA) calculation

Nitrogen-accessible surface areas (NASAs) were calculated geometrically using the method described by Bae *et al.*,[5] where NASAs correspond to the areas of the surface created by the center of a nitrogen-sized *hard* spherical probe when it is rolled over the atoms of the crystal structure of interest. The diameter of the spherical probe and the diameter of the framework atoms are equal to $2^{1/6}$ times the corresponding Lennard Jones (LJ) "σ" parameter. The σ parameter of the spherical probe (3.32 Å) is based on the TraPPE force field of nitrogen,[4] whereas those of the atoms of the investigated materials are based on the Universal Force Field (UFF).[3] Note that although the probe is spherical, it delineates (in principle) the same area covered by the N_2 monolayer as illustrated in the simplified example in **Figure S1.3**, in which adsorption around an isolated carbon atom is considered.

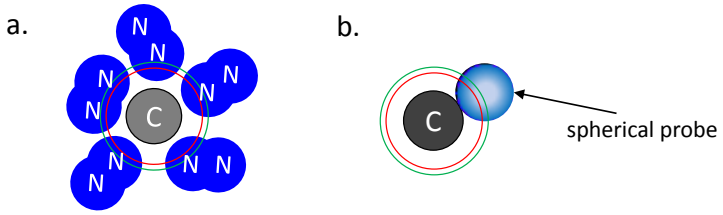

Figure S1.3. (a) Schematic of nitrogen molecule adsorbing around and contacting an isolated carbon atom. The depicted sizes of the N and C atoms (blue and gray, respectively) are equal to σ_N and σ_C, respectively. The red and green circles correspond to $\sigma_{C\text{-}N}$ and $2^{1/6}\sigma_{C\text{-}N}$, respectively. Since nitrogen molecules adsorb (on average) with the relevant N atom center at $2^{1/6}\sigma_{C\text{-}N}$, the area "covered" by the nitrogen molecules corresponds to the green circle. (b) Schematic of a spherical probe rolling around an isolated carbon atom. The depicted sizes of the spherical probe and the C atom are equal to $2^{1/6}\sigma_N$ and $2^{1/6}\sigma_C$, respectively. The red and green circles correspond to $\sigma_{C\text{-}N}$ and $2^{1/6}\sigma_{C\text{-}N}$, respectively. Note that when the probe is rolled around the carbon atom, the probe center delineates the same surface covered by the nitrogen molecules in panel *a* (i.e. green circle).

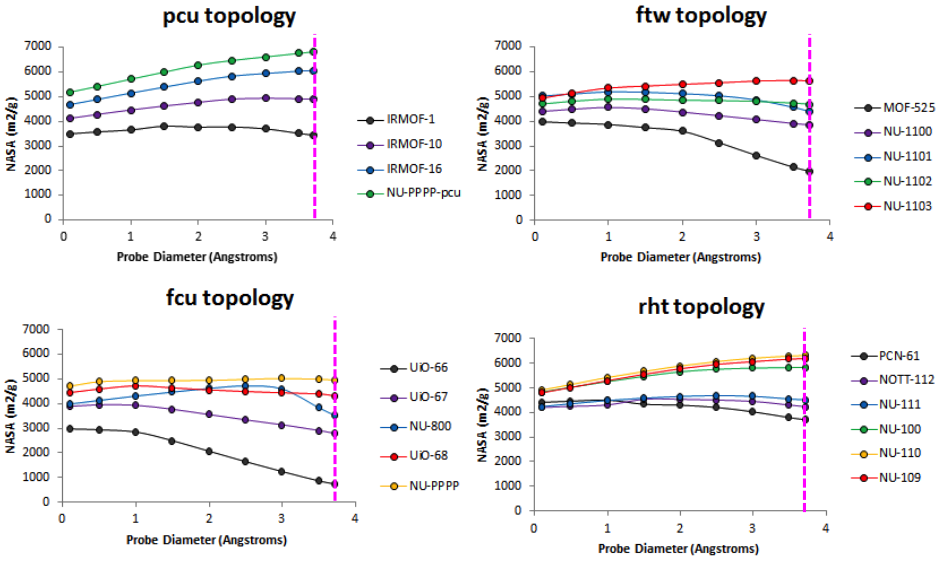

Figure S1.4. Sensitivity of the geometrically calculated NASA to the probe size for MOFs of the four topologies systematically investigated in this work. The vertical pink line indicates the probe size used in this work.

BET area calculation

Once a nitrogen monolayer loading is estimated by applying the BET theory to the simulated nitrogen isotherms, it is converted to a BET area. For this conversion we use:

$$BET\ area = \ N_m \times (V_m)_{STP} \times N_A \times S_{N_2}$$

where N_m is the monolayer loading in "m^3(STP)/$g_{adsorbent}$" units, $(V_m)_{STP}$ is the molar density of nitrogen at standard temperature and pressure (44.6 mol/m^3), N_A is the Avogadro number (6.02 x 10^{23}) and S_{N2} is the effective cross-sectional area of nitrogen (1.62 x 10^{-19} m^2)

Section 2. Pore structure schematics for various topologies

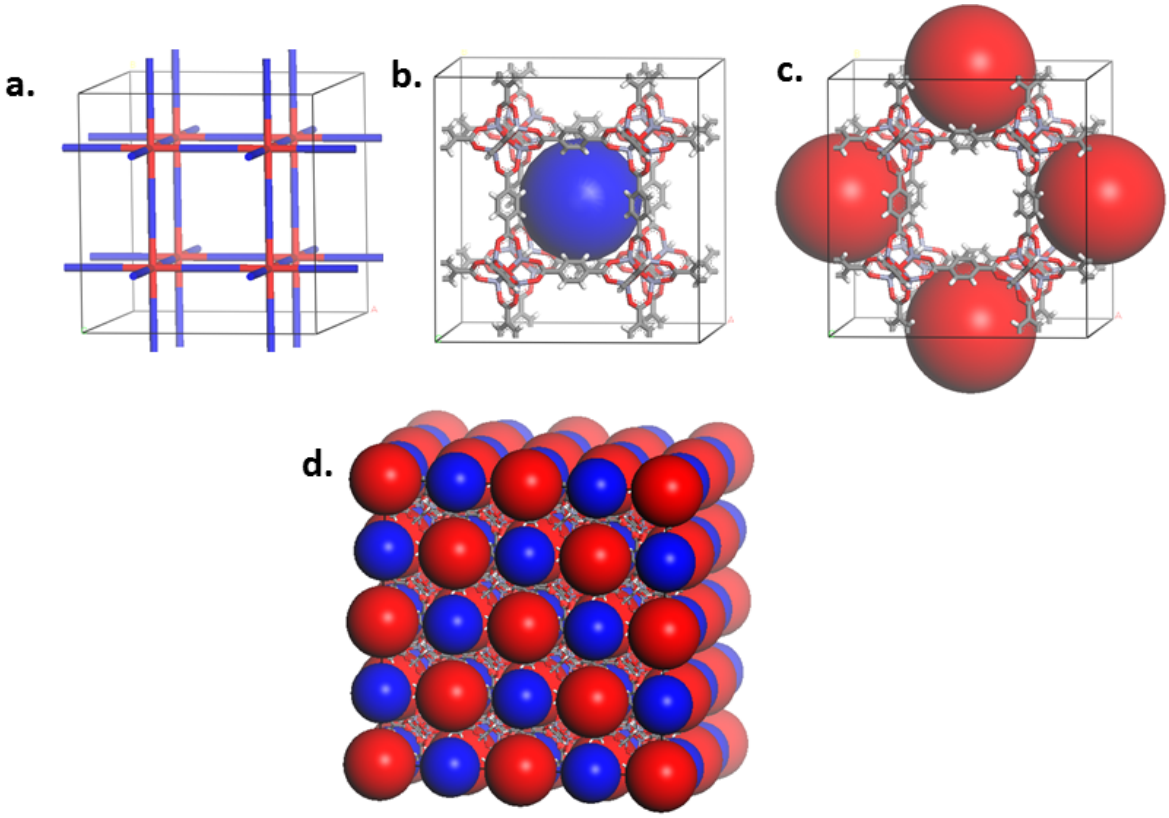

Figure S2.1. a) Schematics of the **pcu** topology. In the structures investigated here, the six-coordinated nodes (red) are occupied by Zn_4O and connected by linkers (blue) of different lengths. Here we investigated the structures **IRMOF-1** (linker with one phenyl ring), **IRMOF-10** (linker with two phenyl rings), **IRMOF-16** (linker with three phenyl rings), and the hypothetical structure pcu-*PPPP* (linker with four phenyl rings). b-d) Illustration of the types of pores found in the **pcu** MOFs studied here using **IRMOF-1** as an example. b) Small cage of **IRMOF-1**. c) Large cage of **IRMOF-1**. d) Complete pore structure of **IRMOF-1** shown in a 2x2x2 supercell.

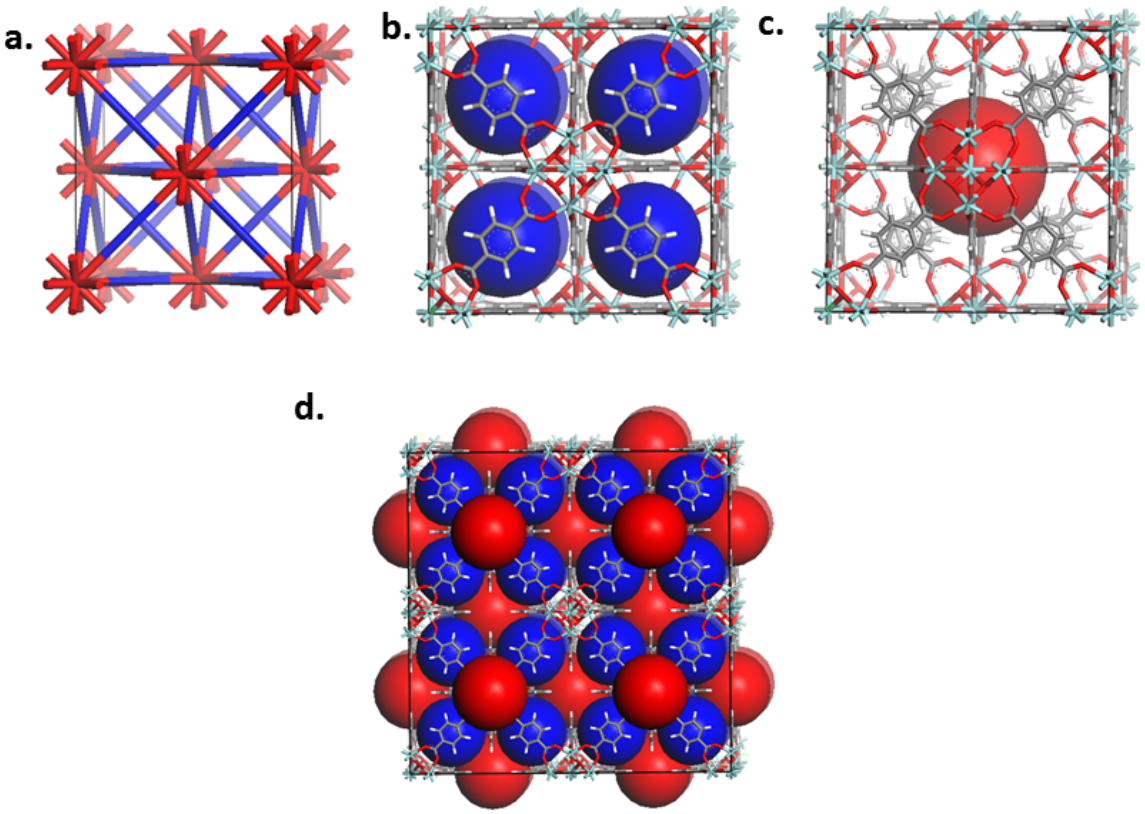

Figure S2.2. a) Schematics of the **fcu** topology. In the structures investigated here, the twelve-coordinated nodes (red) are occupied by Zr_6O_8 nodes, and connected by linkers (blue) of different lengths. Here we investigated the structures **UiO-66** (linker with one phenyl ring), **UiO-67** (linker with two phenyl rings), **NU-800** (linker with two triple bonds "T" and one phenyl ring "P" in the TPT sequence), **UiO-68 (**linker with three phenyl rings**),** and the hypothetical structure fcu-*PPPP* (linker with four phenyl rings). b-d) Illustration of the types of pores found in the **fcu** MOFs studied here using **UiO-66** as an example. b) Tetrahedral cage of **UiO-66**. c) Octahedral cage of **UiO-66**. d) Complete pore structure of **UiO-66** shown in a 2x2x2 supercell.

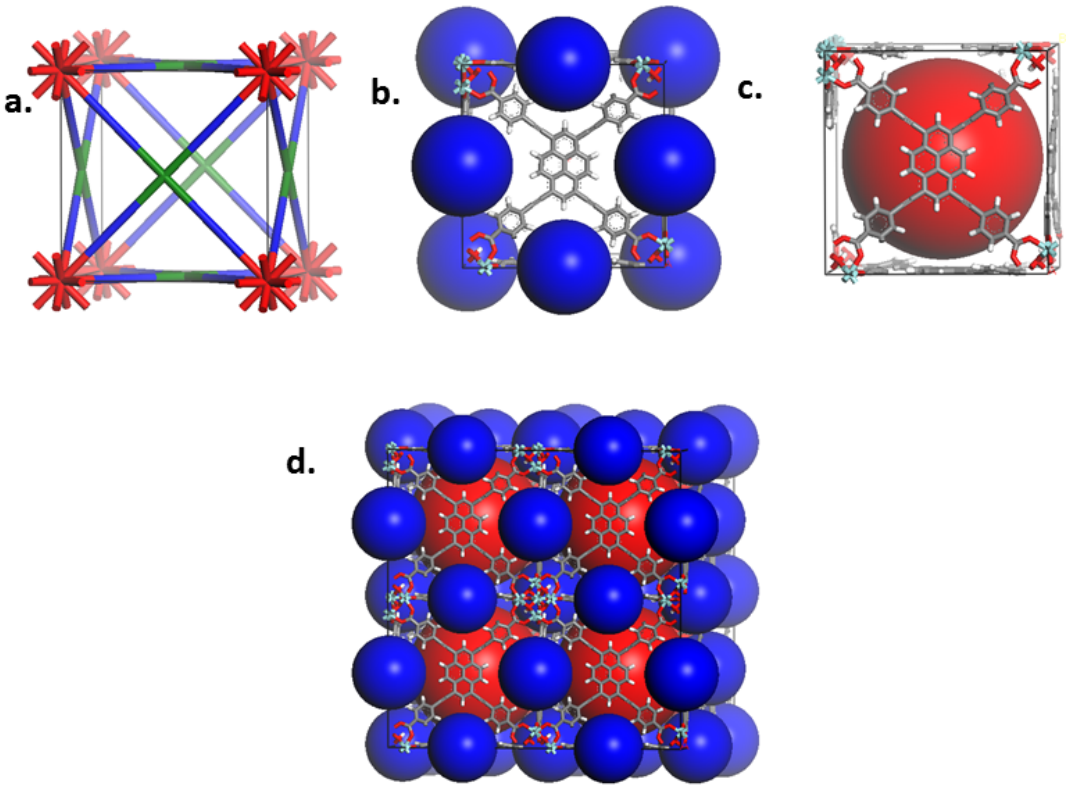

Figure S2.3. a) Schematics of the bimodal **ftw** topology. In the structures investigated here, the twelve-coordinated nodes (red) are occupied by Zr_6O_8 nodes, and the four-coordinated nodes (green) correspond to the central group of the organic linkers and they are occupied with either pyrene or porphyrine moieties. The arms of the organic linkers (blue) can vary in length and they connect the central organic moiety to the inorganic nodes. Here we investigated the structures **MOF-525** (central porphyrine and arms with one phenyl ring), **NU-1100** (central pyrene and arms with one triple bond and one phenyl ring), **NU-1101** (central pyrene and arms with one xylene group and one phenyl ring), **NU-1102** (central porphyrine and arms with two phenyl rings), **NU-1103** (central pyrene and arms with two phenyl (P) rings and one triple (T) bond in "PTP" sequence), and **NU-1104** (central porphyrine and arms with two phenyl (P) rings and one triple (T) bond in "PTP" sequence). b-d) Illustration of the types of pores found in the **ftw** MOFs studied here using **NU-1100** as an example. b) Octahedral cage of **NU-1100**. c) Cubic cage of **NU-1100**. d) Complete pore structure of **NU-1100** shown in a 2x2x2 supercell.

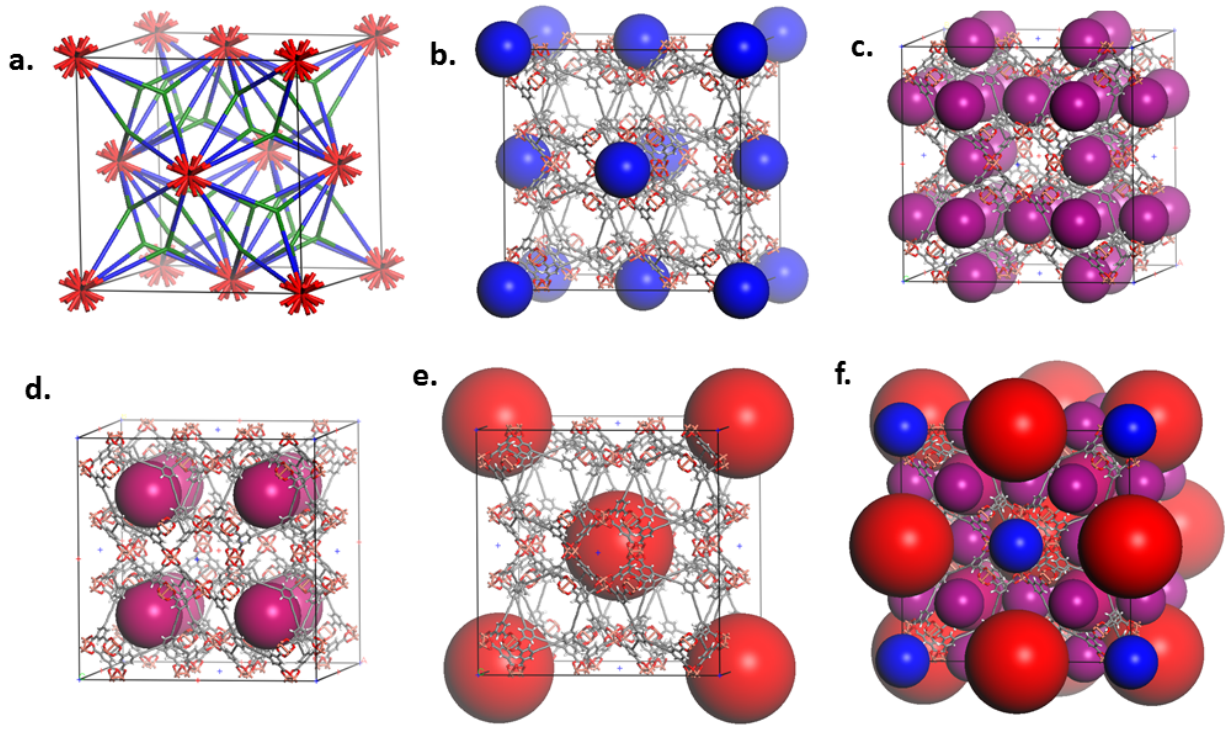

Figure S2.4. a) Schematics of the bimodal **rht** topology. In the structures investigated here, the 24-coordinated nodes (red) are occupied by $[Cu_2(COO)_4]_{12}[C_4H_4]_{24}$ supermolecular cages, and the three-coordinated nodes (green) correspond to the central group of the organic linkers and they are occupied by a phenyl ring. The arms of the organic linkers (blue) can vary in length and they connect the central organic moiety to the supermolecular cages. Here we investigated the structures **PCN-61** (organic linker arms with one triple bond), **NOTT-112** (organic linker arms with one phenyl ring), **NU-111** (organic linker arms with two triple bonds), **NU-100** (organic linker arms with two triple (T) bonds and one phenyl (P) ring in "TPT" sequence), **NU-109** (organic linker arms with three triple (T) bonds and one phenyl (P) ring in "TPTT" sequence), and **NU-110** (organic linker arms with two triple (T) bonds and two phenyl (P) rings in "TPTP" sequence). b-f) Illustration of the types of pores found in the **rht** MOFs studied here using **NU-111** as an example. b) Supermolecular cage of **NU-111**. c) Interstitial cage of **NU-111** d) Tetrahedral cage of **NU-111**. e) Large (octahedral) cage of **NU-111**, f) Complete pore structure of **NU-111** shown in a 1x1x1 supercell.

Section 3. BET calculations

MOFs with fcu topology

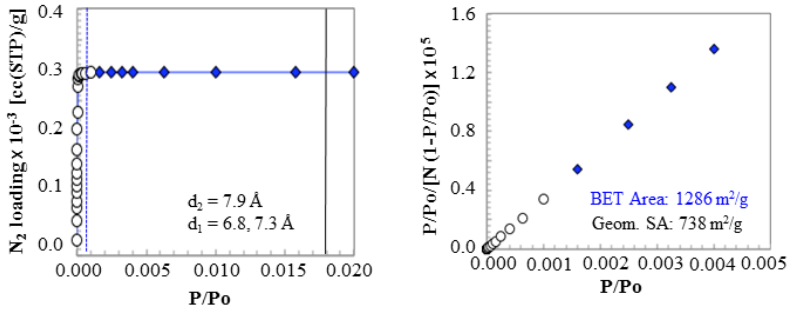

Figure S3.1. BET area calculation for **UiO-66.** Left panel shows the nitrogen isotherms (white symbols indicate points used in calculation; blue vertical dashed lines indicate the P/Po values that correspond to the calculated monolayer loadings; black vertical lines indicate the values of $1/(\sqrt{C}+1)$; inset numbers correspond to geometrically calculated pore sizes). Right panels show the BET plots used for the calculation (all points shown satisfy the first consistency criteria; white symbols indicate points used in calculation).

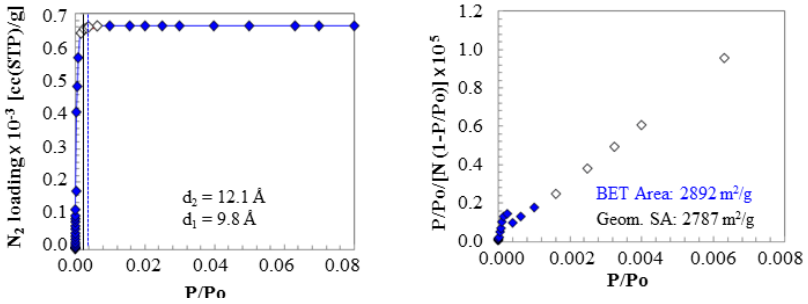

Figure S3.2. BET area calculation for **UiO-67.** See Figure S3.1 for description of the plots.

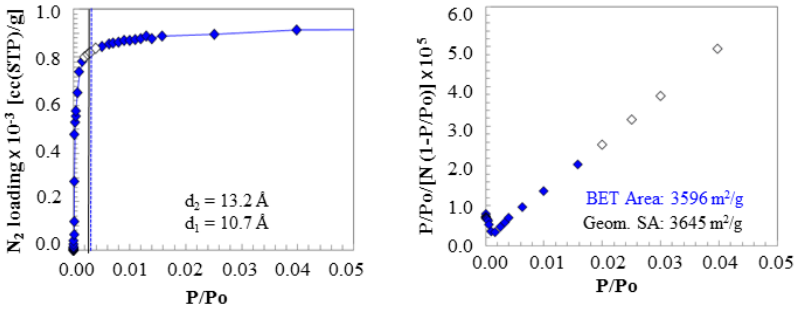

Figure S3.3. BET area calculation for **NU-800.** See Figure S3.1 for description of the plots.

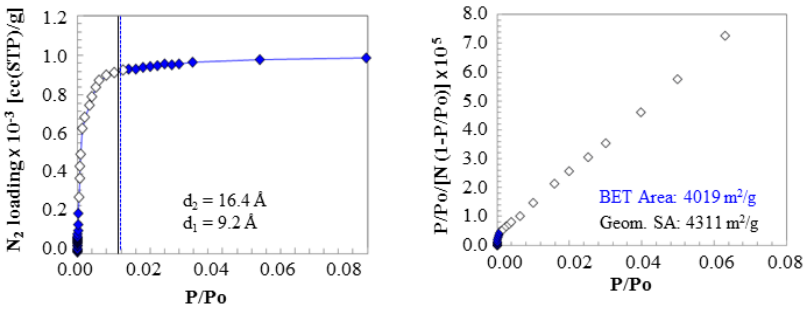

Figure S3.4. BET area calculation for **UiO-68.** See Figure S3.1 for description of the plots.

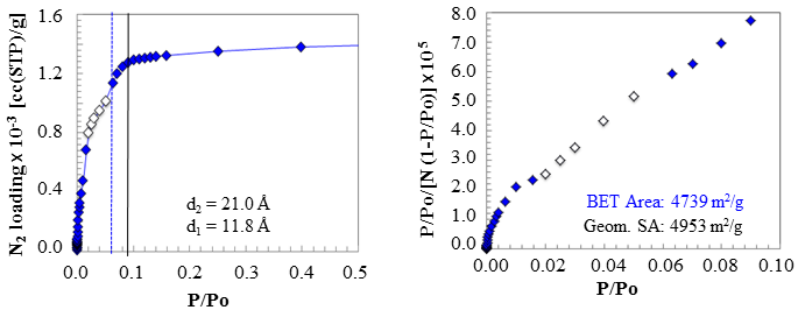

Figure S3.5. BET area calculation for fcu-*PPPP***.** See Figure S3.1 for description of the plots.

MOFs with ftw topology

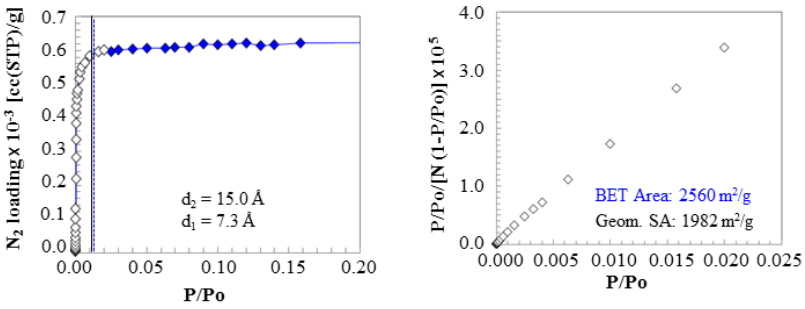

Figure S3.6. BET area calculation for **MOF-525.** Left panel shows the nitrogen isotherms (white symbols indicate points used in calculation; blue vertical dashed lines indicate the P/Po values that correspond to the calculated monolayer loadings; black vertical lines indicate the values of $1/(\sqrt{C}+1)$; inset numbers correspond to geometrically calculated pore sizes). Right panels show the BET plots used for the calculation (all points shown satisfy the first consistency criteria; white symbols indicate points used in calculation).

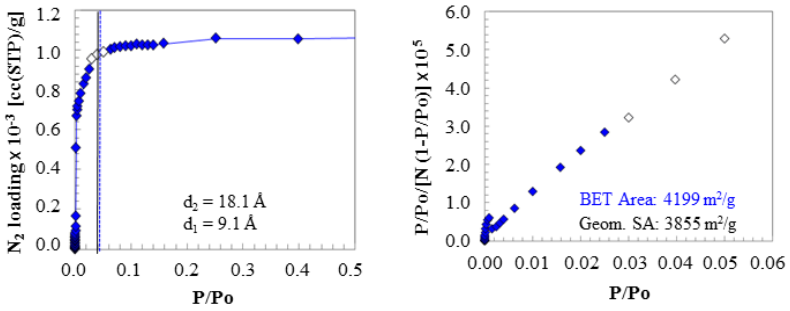

Figure S3.7. BET area calculation for **NU-1100.** See Figure S3.6 for description of the plots.

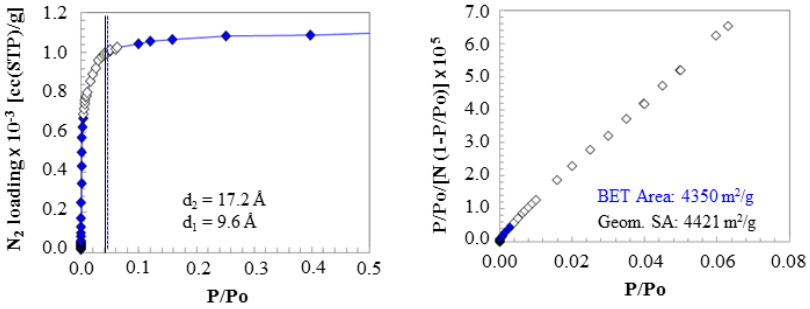

Figure S3.8. BET area calculation for **NU-1101.** See Figure S3.6 for description of the plots.

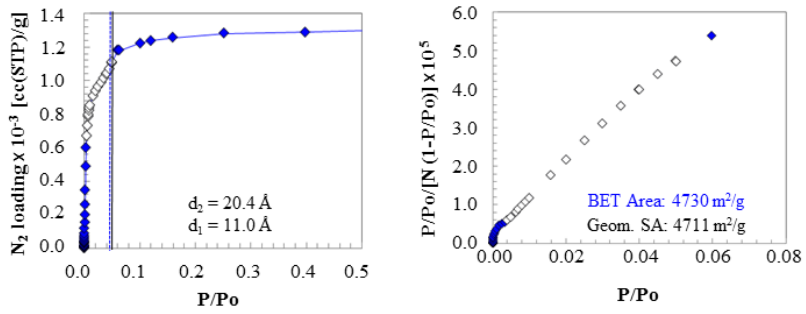

Figure S3.9. BET area calculation for **NU-1102.** See Figure S3.6 for description of the plots.

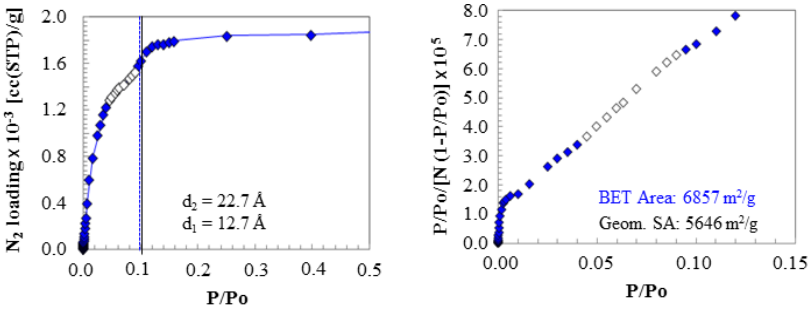

Figure S3.10. BET area calculation for **NU-1103.** See Figure S3.6 for description of the plots

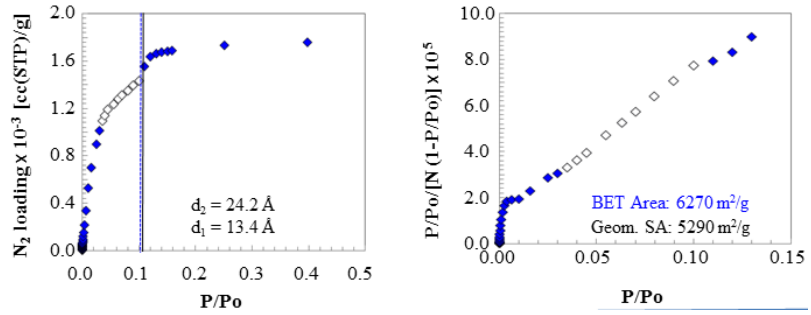

Figure S3.11. BET area calculation for **NU-1104.** See Figure S3.6 for description of the plots.

MOFs with rht topology

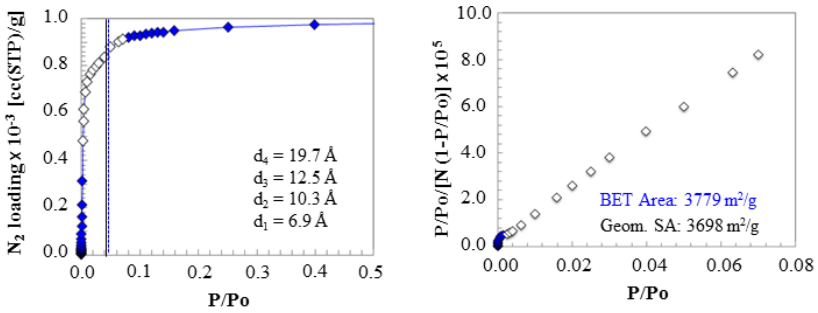

Figure S3.12. BET area calculation for **PCN-61.** Left panel shows the nitrogen isotherms (white symbols indicate points used in calculation; blue vertical dashed lines indicate the P/Po values that correspond to the calculated monolayer loadings; black vertical lines indicate the values of $1/(\sqrt{C}+1)$; inset numbers correspond to geometrically calculated pore sizes). Right panels show the BET plots used for the calculation (all points shown satisfy the first consistency criteria; white symbols indicate points used in calculation).

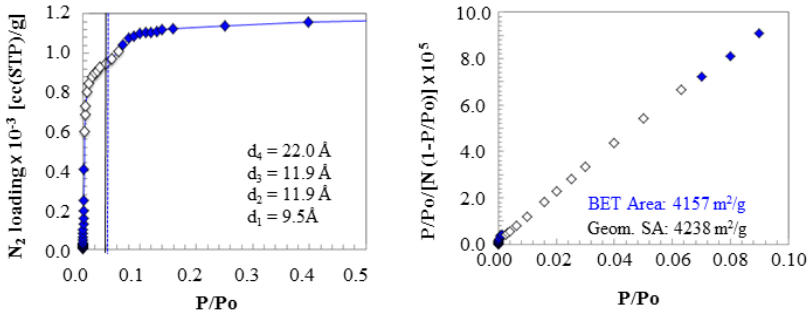

Figure S3.13. BET area calculation for **NOTT-112.** See Figure S3.12 for description of the plots.

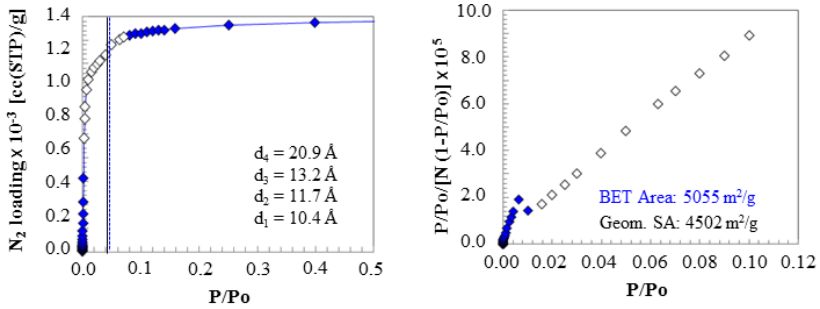

Figure S3.14. BET area calculation for **NU-111.** See Figure S3.12 for description of the plots.

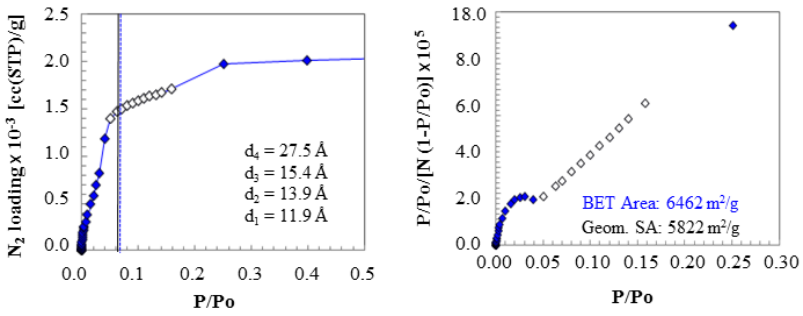

Figure S3.15. BET area calculation for **NU-100.** See Figure S3.12 for description of the plots.

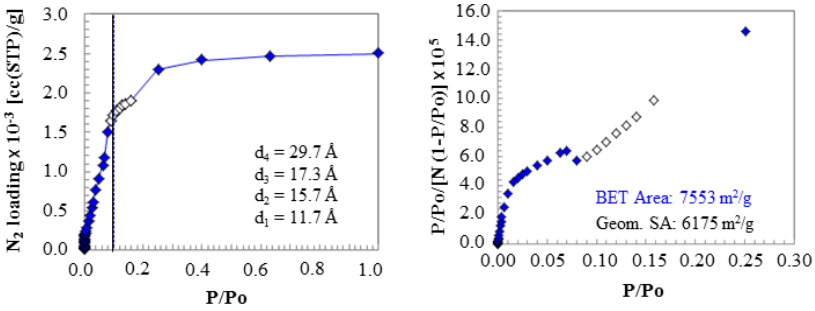

Figure S3.16. BET area calculation for **NU-109.** See Figure S3.12 for description of the plots.

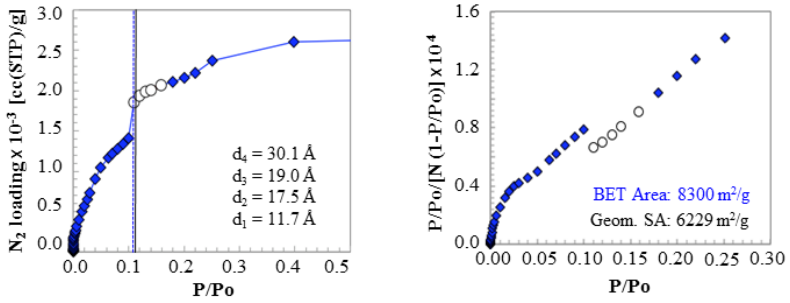

Figure S3.17. BET area calculation for **NU-110.** See Figure S3.12 for description of the plots.

MOFs with pcu topology

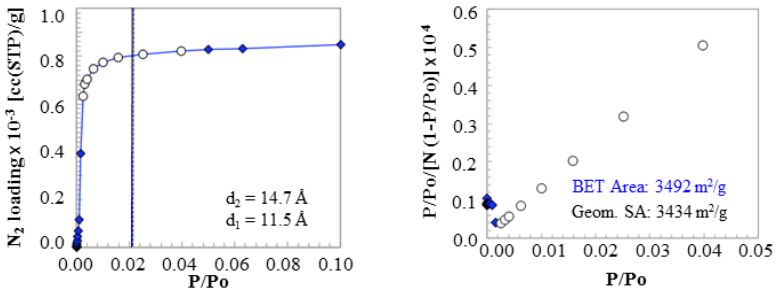

Figure S3.18. BET area calculation for **IRMOF-1.** Left panel shows the nitrogen isotherms (white symbols indicate points used in calculation; blue vertical dashed lines indicate the P/Po values that correspond to the calculated monolayer loadings; black vertical lines indicate the values of $1/(\sqrt{C}+1)$; inset numbers correspond to geometrically calculated pore sizes). Right panels show the BET plots used for the calculation (all points shown satisfy the first consistency criteria; white symbols indicate points used in calculation).

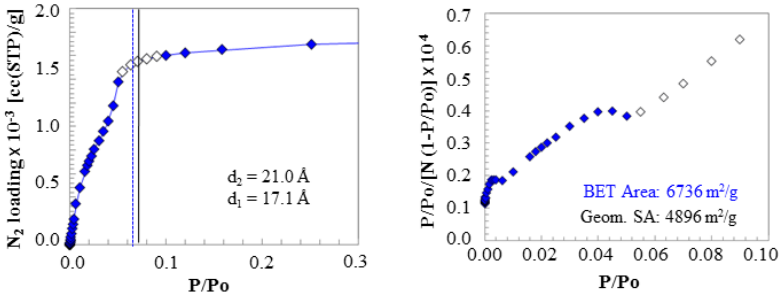

Figure S3.19. BET area calculation for **IRMOF-10.** See Figure S3.18 for description of the plots.

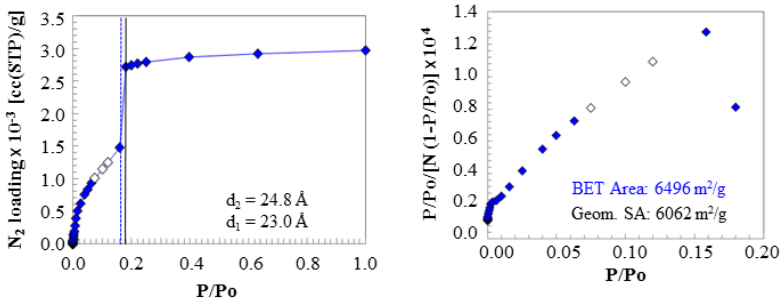

Figure S3.20. BET area calculation for **IRMOF-16.** See Figure S3.18 for description of the plots.

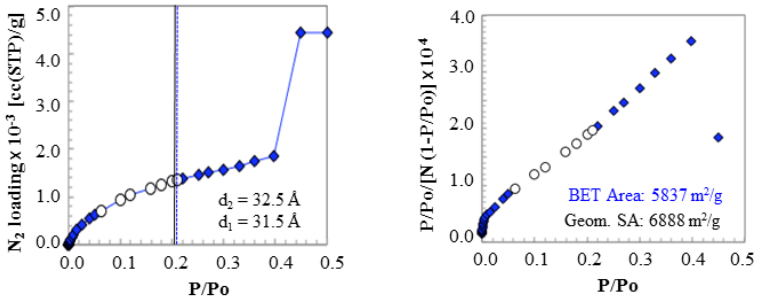

Figure S3.21. BET area calculation for pcu-*PPPP*. See Figure S3.18 for description of the plots.

MOFs with other topologies

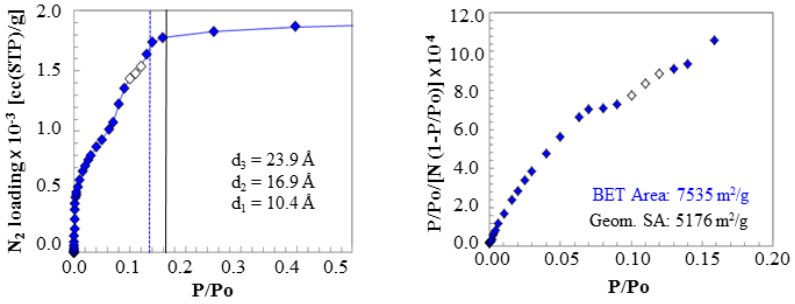

Figure S3.22. BET area calculation for **DUT-49.** Left panel shows the nitrogen isotherms (white symbols indicate points used in calculation; blue vertical dashed lines indicate the P/Po values that correspond to the calculated monolayer loadings; black vertical lines indicate the values of $1/(\sqrt{C}+1)$; inset numbers correspond to geometrically calculated pore sizes). Right panels show the BET plots used for the calculation (all points shown satisfy the first consistency criteria; white symbols indicate points used in calculation).

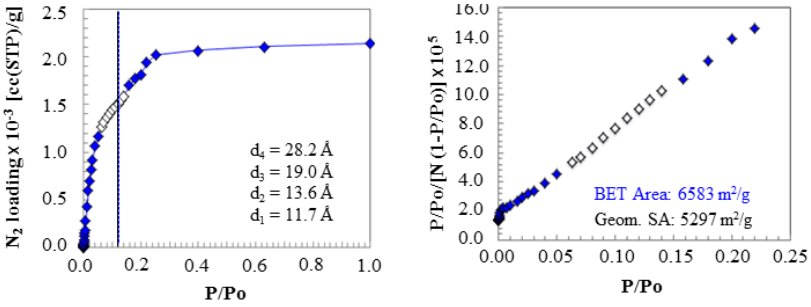

Figure S3.23. BET area calculation for **DUT-32.** See Figure S3.22 for description of the plots.

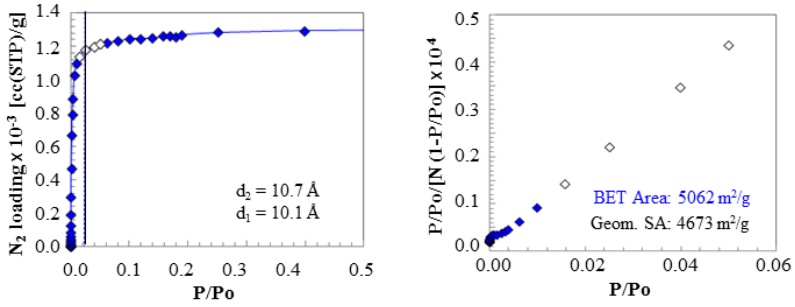

Figure S3.24. BET area calculation for **MOF-177.** See Figure S3.22for description of the plots.

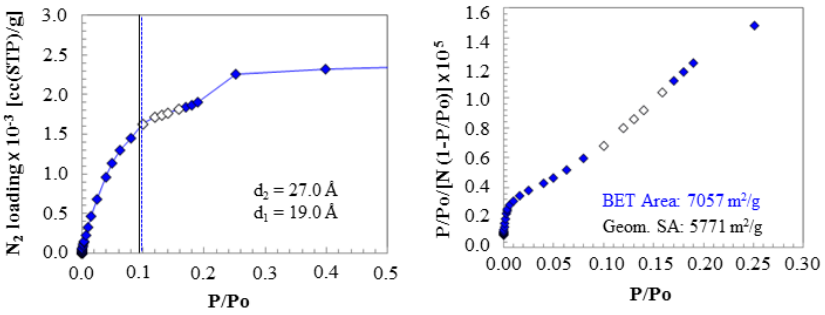

Figure S3.25. BET area calculation for **MOF-210.** See Figure S3.22 for description of the plots.

Graphene systems

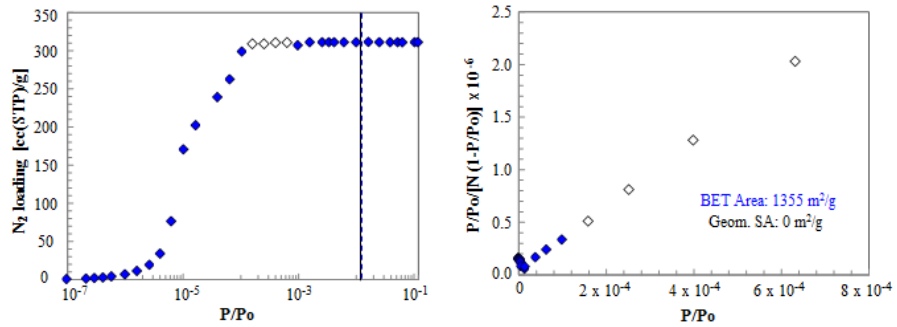

Figure S3.26. BET area calculation for **graphene layers with pore diameter of 3.2 Å.** Left panel shows the nitrogen isotherms (white symbols indicate points used in calculation; blue vertical dashed lines indicate the P/Po values that correspond to the calculated monolayer loadings; black vertical lines indicate the values of $1/(\sqrt{C}+1)$; inset numbers correspond to geometrically calculated pore sizes). Right panels show the BET plots used for the calculation (all points shown satisfy the first consistency criteria; white symbols indicate points used in calculation).

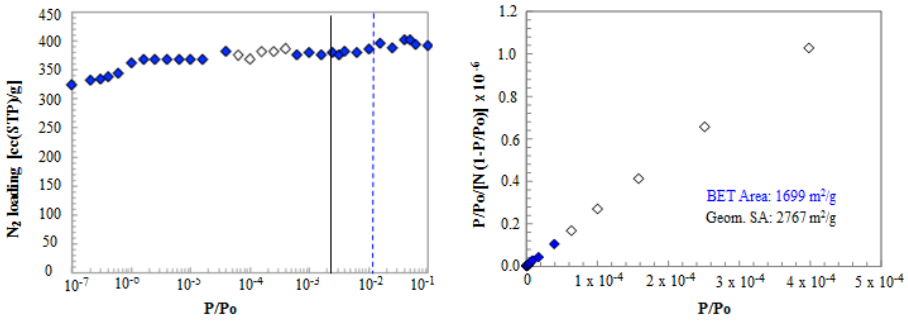

Figure S3.27. BET area calculation for **graphene layers with pore diameter of 5.2 Å.** See Figure S3.26 for description of the plots.

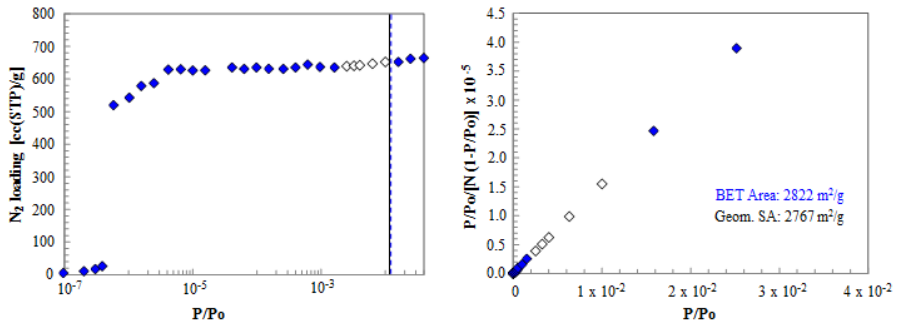

P/Po range	BET area m^2/g	N_2@ lower P/Po cc(STP)/g	BET predicted monolayer cc(STP)/g	N_2@ upper P/Po cc(STP)/g	3rd criterion fulfilled?	C	1/(VC + 1)	BET monolayer P/Po	4th criterion % error	BET criteria fullfilled?
0.0000063-0.02510	2805	629	644	661	Yes	77621	0.00357	0.0071	-50	No
0.0025-0.02510	2810	639	645	661	Yes	28388	0.0059	0.0075	-21	No
0.0000006-0.0000040	2839	519	652	628	No	5112640	0.000442	0.0099	-96	No
0.0025-0.01	2822	639	648	652	Yes	17341	0.0075	0.007	7	Yes

Figure S3.28. BET area calculation for **graphene layers with pore diameter of 6.9 Å.** See Figure S3.26 for description of the plots. The bottom table shows different pressure ranges investigated for BET calculations. Notice that the calculated BET areas are insensitive to either third or fourth consistency criterion.

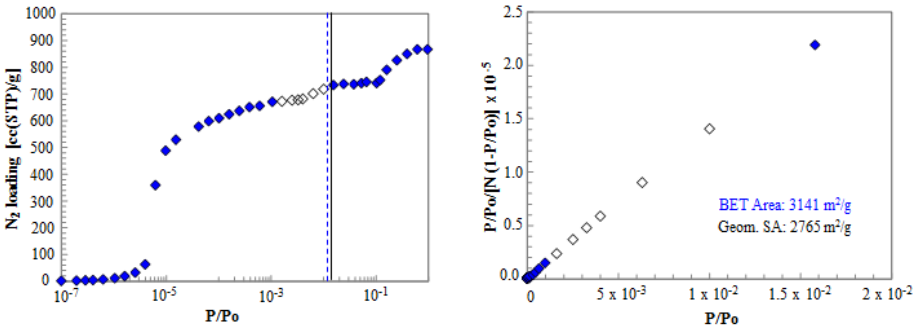

Figure S3.29. BET area calculation for **graphene layers with pore diameter of 8.9 Å.** See Figure S3.26 for description of the plots

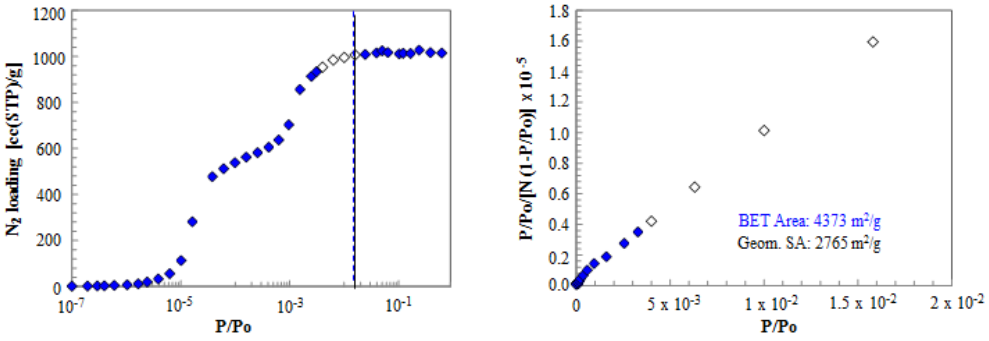

Figure S3.30. BET area calculation for **graphene layers with pore diameter of 10.9 Å.** See Figure S3.26 for description of the plots.

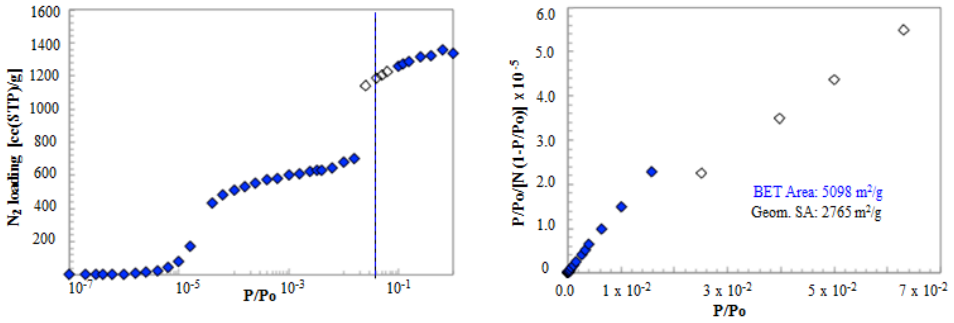

P/Po range	BET area m^2/g	N_2@ lower P/Po cc(STP)/g	BET predicted monolayer cc(STP)/g	N_2@ upper P/Po cc(STP)/g	3rd criterion fulfilled?	C	1/(VC + 1)	BET monolayer P/Po	4th criterion % error	BET criteria fullfilled?
0.004-0.0158	*3113*	*633*	*715*	*700*	*No*	*1627*	*0.02419*	*0.016*	*51*	*No*
0.000631-0.0025	*2776*	*582*	*637*	*624*	*No*	*15687*	*0.00792*	*0.0046*	*69*	*No*
0.025-0.063	5098	1140	1171	1225	Yes	791	0.0343	0.034	0.98	Yes

Figure S3.31. BET area calculation for **graphene layers with pore diameter of 13.2 Å.** See Figure S3.26 for description of the plot. The bottom table shows different pressure ranges investigated for BET calculations. Notice that the calculated BET areas corresponding to the first linear region (italic data) agree very well with the NASA but do not satisfy the third and fourth criteria.

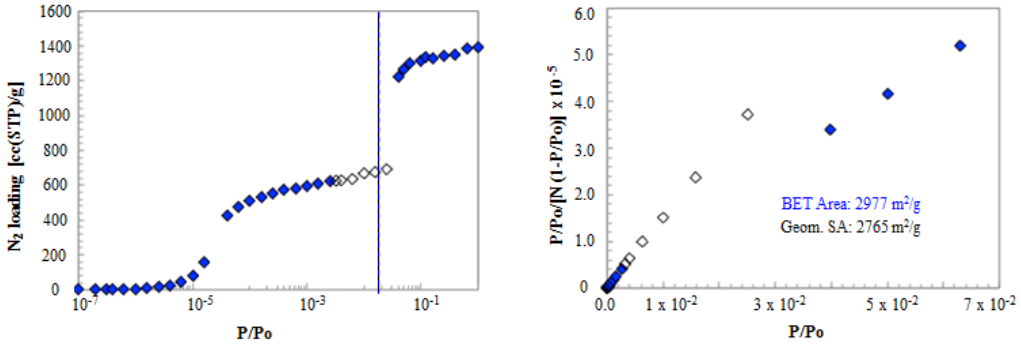

Figure S3.32. BET area calculation for **graphene layers with pore diameter of 14.7 Å.** See Figure S3.26 for description of the plots.

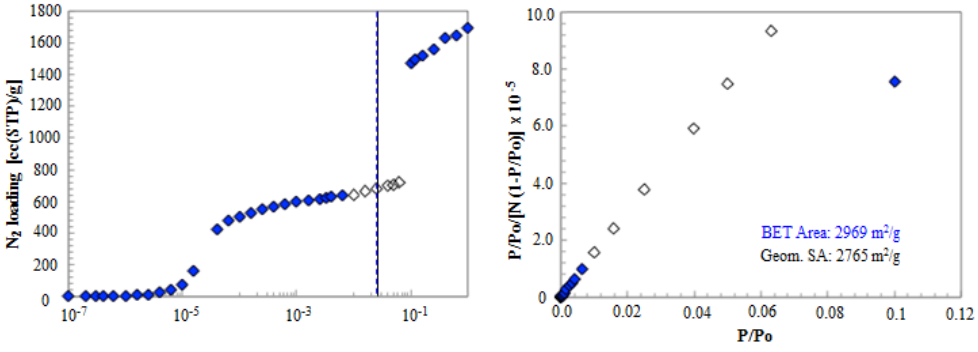

Figure S3.33. BET area calculation for **graphene layers with pore diameter of 16.8 Å.** See Figure S3.26 for description of the plots.

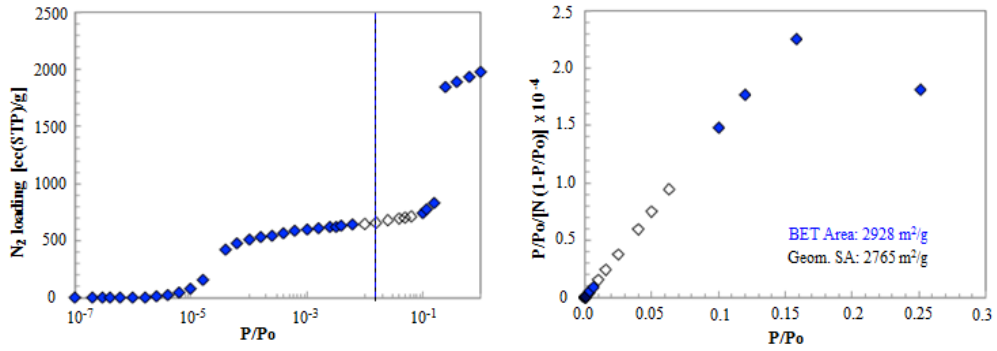

Figure S3.34. BET area calculation for **graphene layers with pore diameter of 20.7 Å.** See Figure S3.26 for description of the plots.

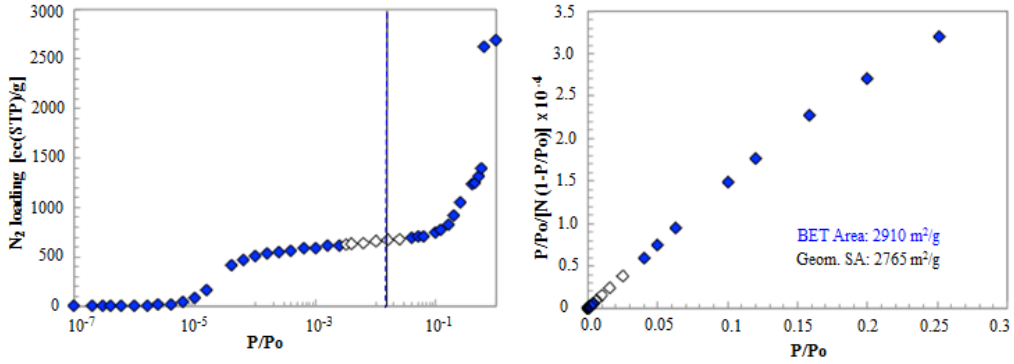

Figure S3.35. BET area calculation for **graphene layers with pore diameter of 29.5 Å.** See Figure S3.26 for description of the plots.

Table S3.1. Comparison between BET areas obtained from simulated nitrogen isotherms calculated using UFF and Dreiding force field (DFF)

Structure	BET area (m^2/g) from "UFF" nitrogen isotherm	BET area (m^2/g) from "DFF" nitrogen isotherm
Graphene (d = 3.2 Å)	1355	1460
Graphene (d = 5.2 Å)	1699	1701
Graphene (d = 6.9 Å)	2822	2850
Graphene (d = 8.9 Å)	3141	3167
Graphene (d = 10.9 Å)	4373	4381
Graphene (d = 13.2 Å)	5098	5134
Graphene (d = 14.7 Å)	2977	2973
Graphene (d = 16.8 Å)	2969	2965
Graphene (d = 20.7 Å)	2928	2948
Graphene (d = 29.5 Å)	2910	2814
IRMOF-1	3490	3464
IRMOF-10	6700	6514
IRMOF-16	6500	6682
pcu-*PPPP*	5837	5004
MOF-525	2560	2407
NU-1100	4200	4163
NU-1101	4350	4169
NU-1102	4730	4832
NU-1103	6860	6960
NU-1104	6270	6262
UiO-66	1290	1281
UiO-67	2900	2988
NU-800	3645	3543
UiO-68	4020	3766
fcu-*PPPP*	4750	5135
PCN-61	3780	3779
NOTT-112	4160	4157
NU-111	5050	5055
NU-100	6460	6371
NU-109	7552	7500
NU-110	8310	8007
DUT-32	6583	6636
DUT-49	7550	7914
MOF-210	7057	7001
MOF-177	5062	4999

Section 4. Curves tracking monolayer formation

MOFs with fcu topology

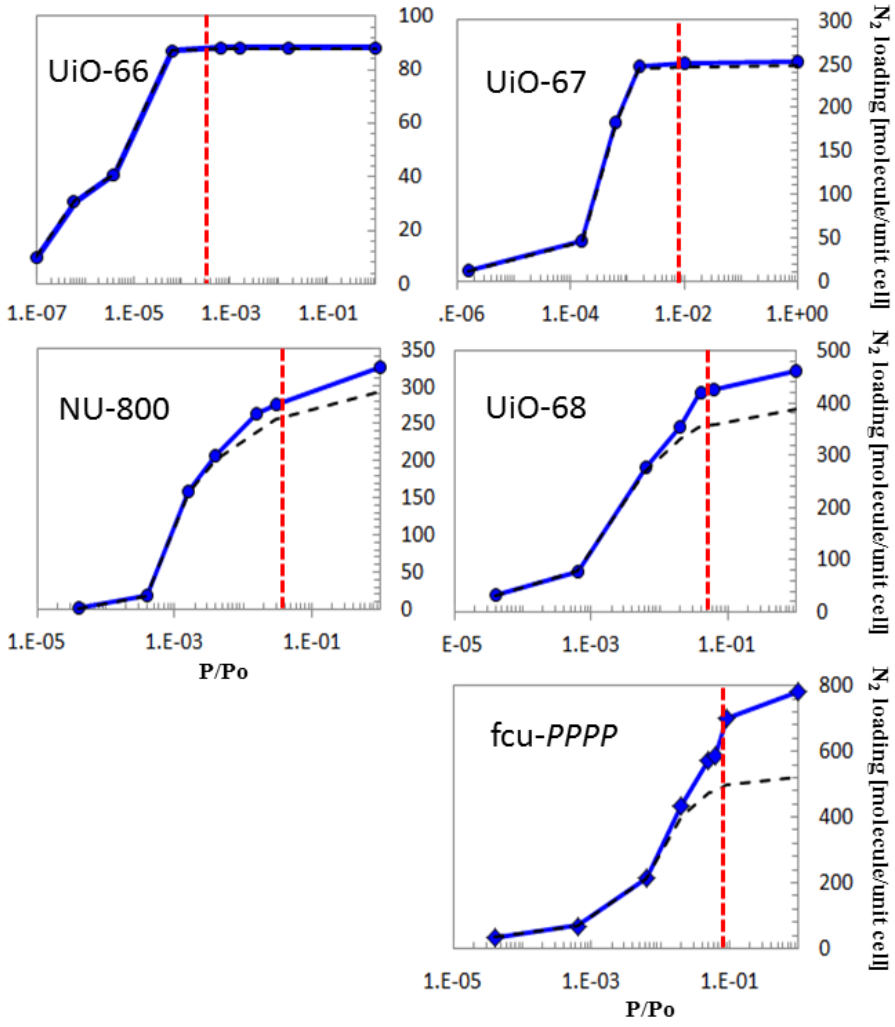

Figure S4.1. Breakdown of total number of nitrogen molecules adsorbed (blue solid curve) and number of nitrogen molecules in contact with pore walls (black dashed curve) for **fcu** MOFs. The dashed black curve tracks the formation of the monolayer. The red vertical dashed line indicates the pressure corresponding to the formation of the monolayer based on the BET calculation.

MOFs with ftw topology

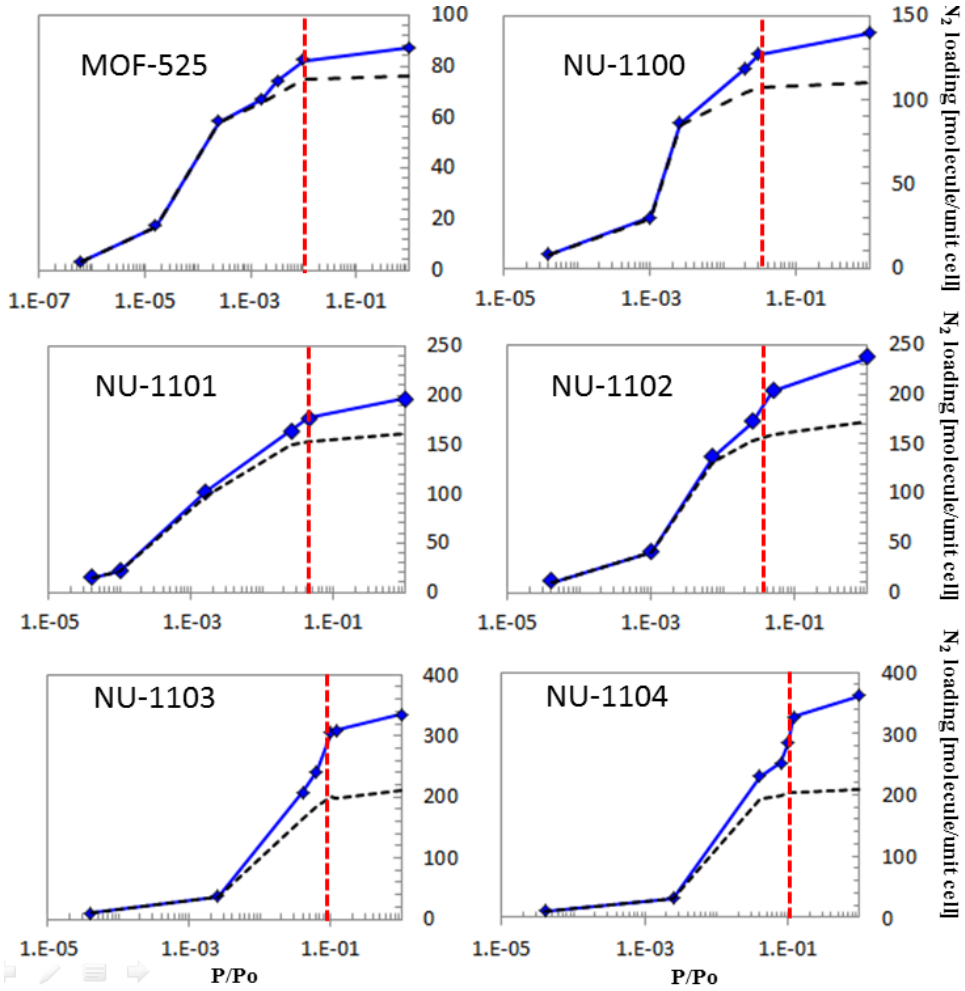

Figure S4.2. Breakdown of total number of nitrogen molecules adsorbed (blue solid curve) and number of nitrogen molecules in contact with pore walls (black dashed curve) for **ftw** MOFs. The dashed black curve tracks the formation of the monolayer. The red vertical dashed line indicates the pressure corresponding to the formation of the monolayer based on the BET calculation.

MOFs with rht topology

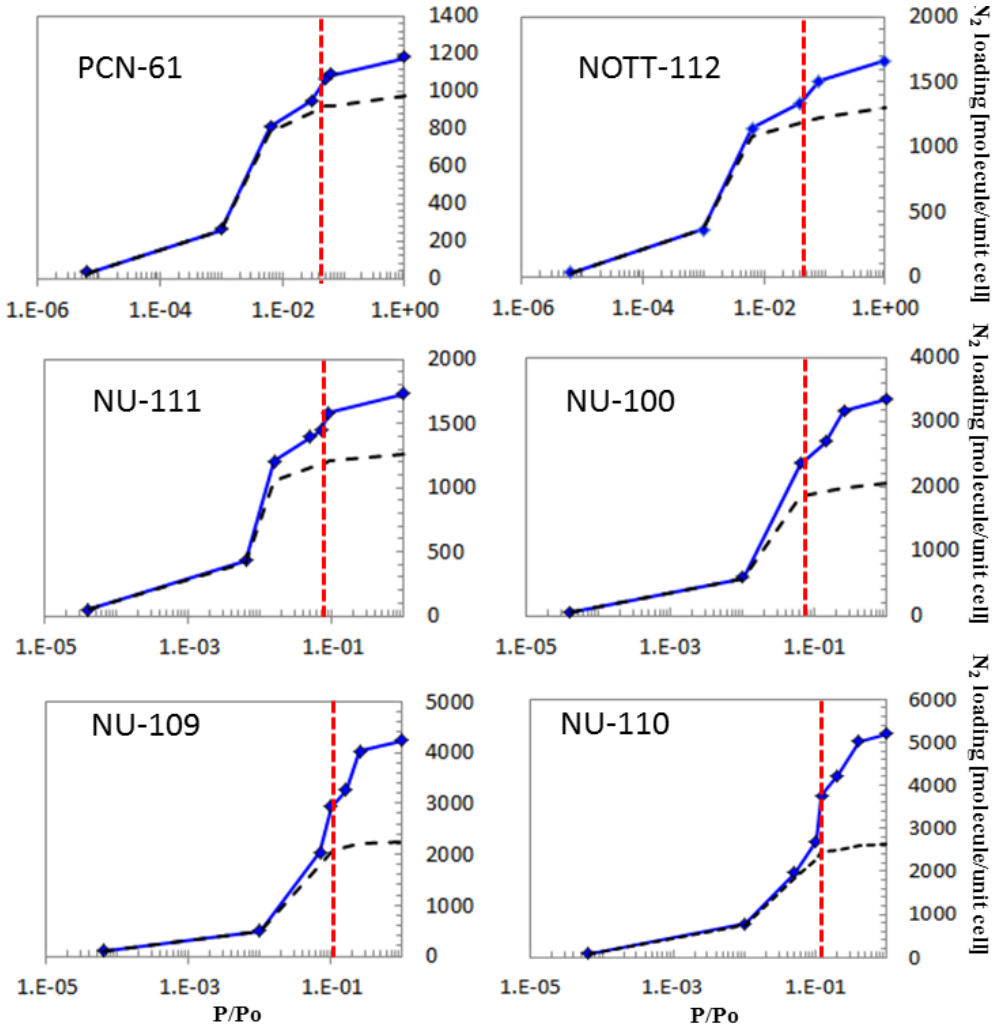

Figure S4.3. Breakdown of total number of nitrogen molecules adsorbed (blue solid curve) and number of nitrogen molecules in contact with pore walls (black dashed curve) for **rht** MOFs. The dashed black curve tracks the formation of the monolayer. The red vertical dashed line indicates the pressure corresponding to the formation of the monolayer based on the BET calculation.

MOFs with pcu topology

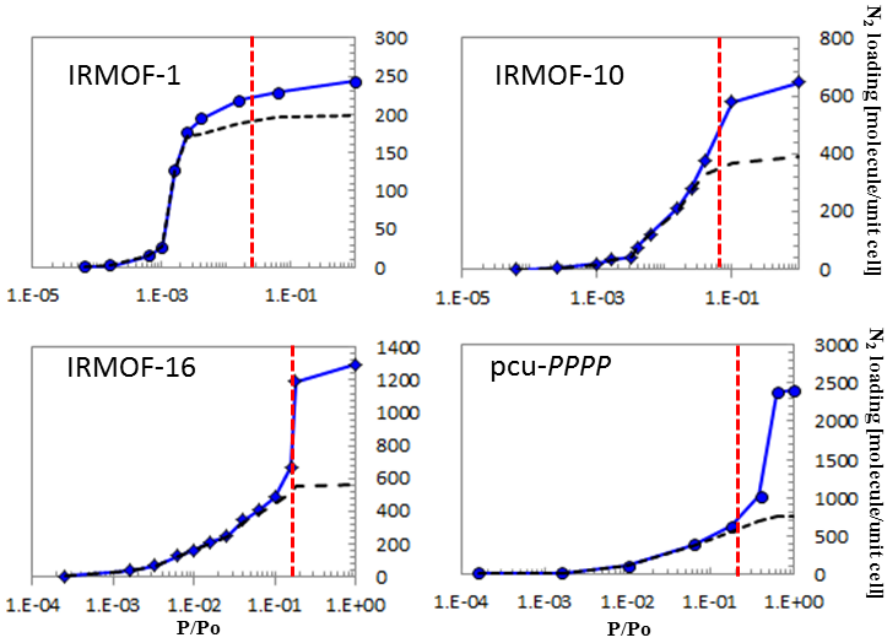

Figure S4.4. Breakdown of total number of nitrogen molecules adsorbed (blue solid curve) and number of nitrogen molecules in contact with pore walls (black dashed curve) for **pcu** MOFs. The dashed black curve tracks the formation of the monolayer. The red vertical dashed line indicates the pressure corresponding to the formation of the monolayer based on the BET calculation.

MOFs with other topologies

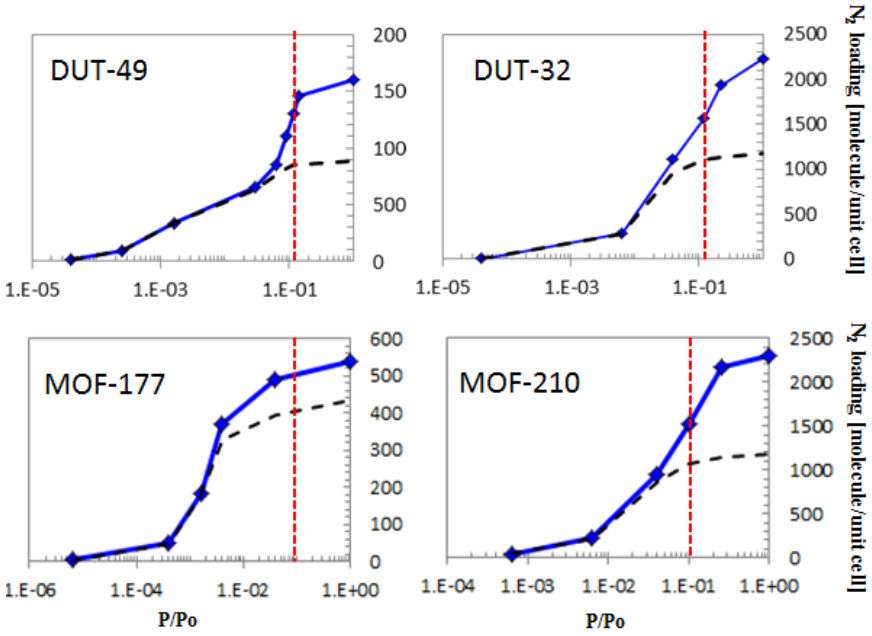

Figure S4.5. Breakdown of total number of nitrogen molecules adsorbed (blue solid curve) and number of nitrogen molecules in contact with pore walls (black dashed curve) for MOFs of other topologies (**umt**: MOF-210 and DUT-32, **ubt**: DUT-49, and **qom**: MOF-177). The dashed black curve tracks the formation of the monolayer. The red vertical dashed line indicates the pressure corresponding to the formation of the monolayer based on the BET calculation.

Section 5. Adsorption loading breakdown by cage types

MOFs with fcu topology

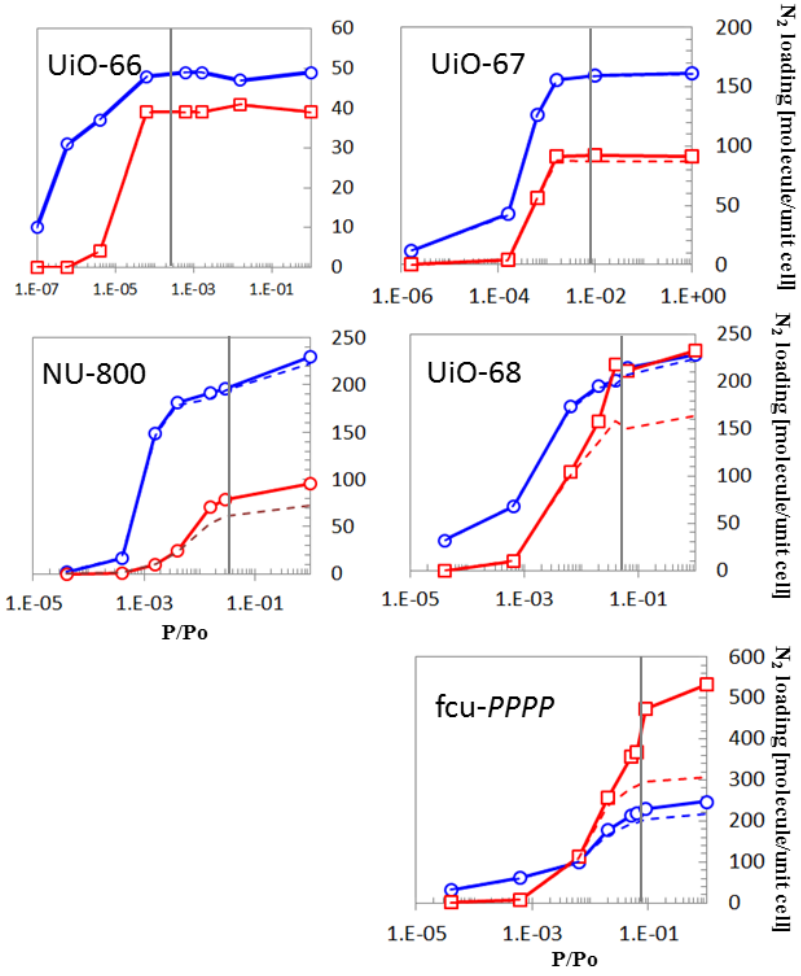

Figure S5.1. Breakdown of total number of nitrogen molecules adsorbed (solid curves) and number of nitrogen molecules in contact with pore walls (dashed curves) for **fcu** MOFs. The red curves (solid and dashed) correspond to adsorption in the octahedral cages, and the blue curves (solid and dashed) correspond to adsorption in the tetrahedral cages. Colors match pore schematics in Figure S2.2. The dashed curves track the formation of the monolayer in the corresponding cages. The vertical line indicates the pressure corresponding to the formation of the monolayer based on the BET calculation.

MOFs with ftw topology

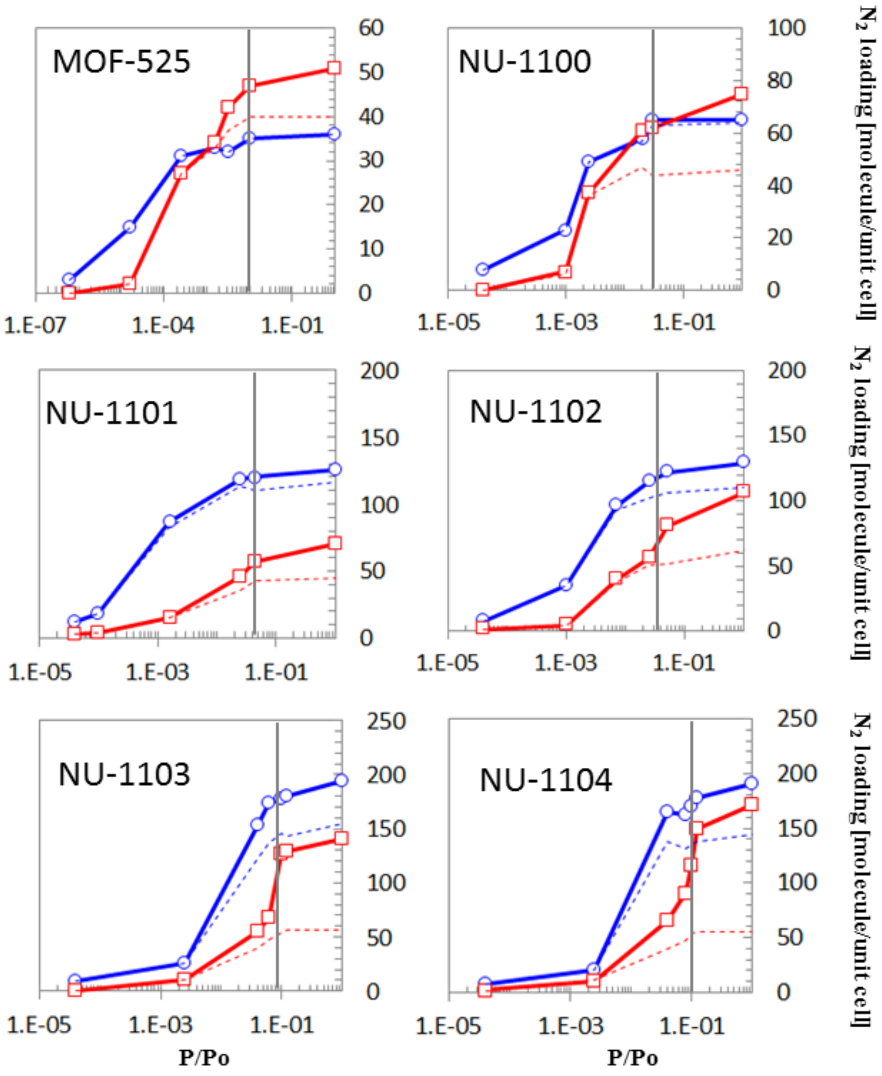

Figure S5.2. Breakdown of total number of nitrogen molecules adsorbed (solid curves) and number of nitrogen molecules in contact with pore walls (dashed curves) for **ftw** MOFs. The red curves (solid and dashed) correspond to adsorption in the cubic cages, and the blue curves (solid and dashed) correspond to adsorption in the octahedral cages. Colors match pore schematics in Figure S2.3. The dashed curves track the formation of the monolayer in the corresponding cages. The vertical line indicates the pressure corresponding to the formation of the monolayer based on the BET calculation.

MOFs with rht topology

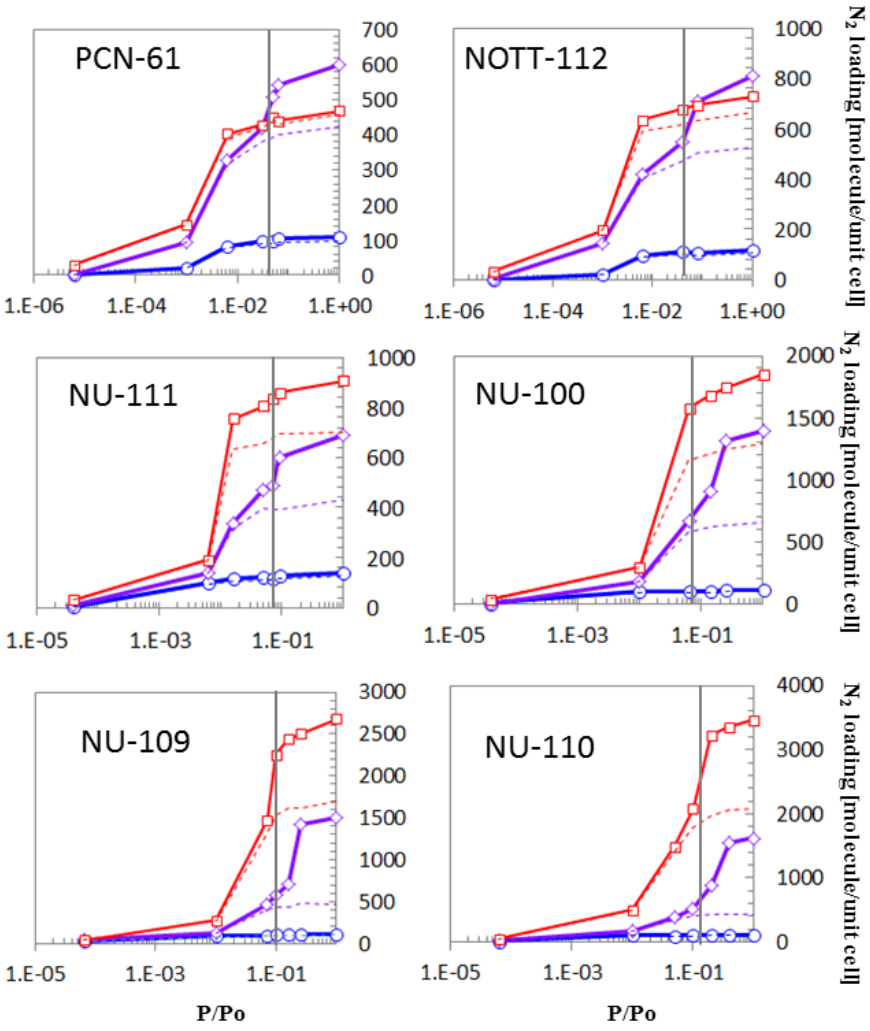

Figure S5.3. Breakdown of total number of nitrogen molecules adsorbed (solid curves) and number of nitrogen molecules in contact with pore walls (dashed curves) for **rht** MOFs. The red curves (solid and dashed) correspond to adsorption in the octahedral cages, the blue curves (solid and dashed) correspond to adsorption in the supermolecular cages, and purple curves correspond to the interstitial and tetrahedral cages. Colors match pore schematics in Figure S2.4. The dashed curves track the formation of the monolayer in the corresponding cages. The vertical line indicates the pressure corresponding to the formation of the monolayer based on the BET calculation.

MOFs with pcu topology

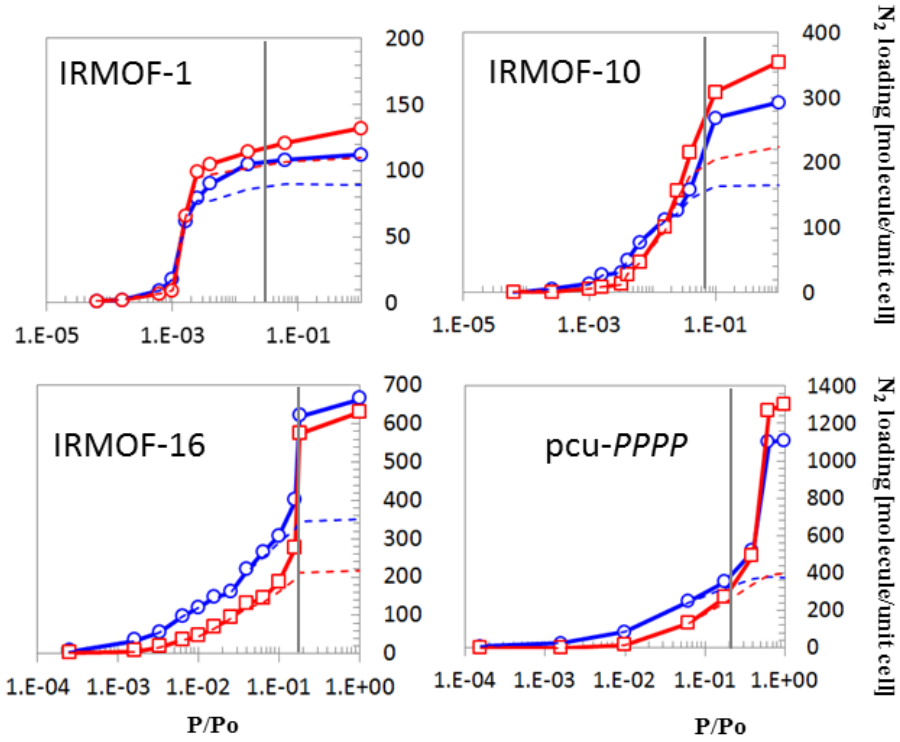

Figure S4.4. Breakdown of total number of nitrogen molecules adsorbed (solid curves) and number of nitrogen molecules in contact with pore walls (dashed curves) for **fcu** MOFs. The red curves (solid and dashed) correspond to adsorption in the larger cages, and the blue curves (solid and dashed) correspond to adsorption in the smaller cages. Colors match pore schematics in Figure S2.1. The dashed curves track the formation of the monolayer in the corresponding cages. The vertical line indicates the pressure corresponding to the formation of the monolayer based on the BET calculation.

Section 6: Example of nitrogen probe inaccessibility in UiO-66

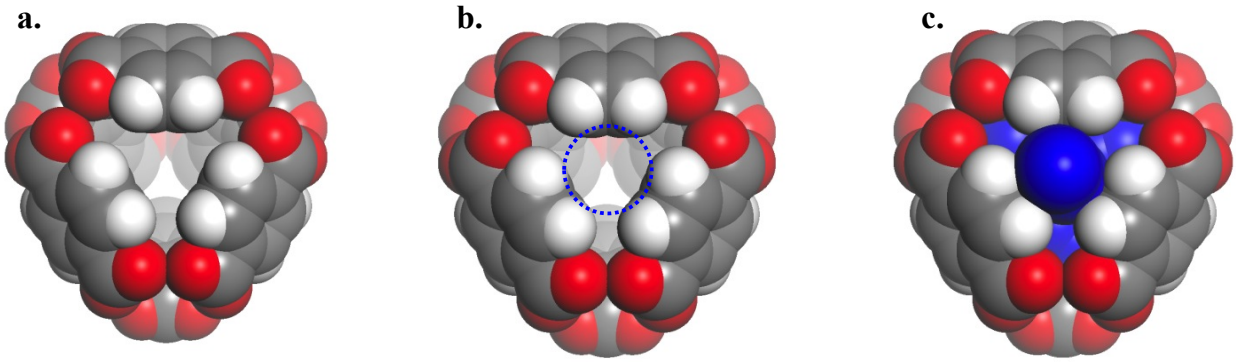

Figure S6.1. Example of regions inaccessible for the hard spherical probe, but accessible for the soft nitrogen molecules. a) Snapshot of a pore window of **UiO-66**, b) Illustration of the overlap of nitrogen spherical probe (dashed circle; d=3.72 Å) with the **UiO-66** window atoms, and c) GCMC simulation snapshot illustrating how "soft" nitrogen molecules access locations at the pore window of **UiO-66** that are not accessible for the hard spherical probe. The size of all atoms is shown as $2^{1/6}\sigma$ in consistency with sizes used for the geometric calculation of nitrogen-accessible surface areas (NASAs).

REFERENCES

(1) Dubbeldam, D.; Calero, S.; Ellis, D. E.; Snurr, R. Q. RASPA: Molecular Simulation Software for Adsorption and Diffusion in Flexible Nanoporous Materials *Mol. Sim.* 2016, 42,-81.

(2) Allen, M. P.; Tildesley, D. J. *Computer Simulation of Liquids*; Oxford University Press: Oxford, 1990.

(3) Rappe, A. K.; Casewit, C. J.; Colwell, K. S.; Goddard, W. A.; Skiff, W. M. Uff, a Full Periodic Table Force Field for Molecular Mechanics and Molecular Dynamics Simulations *J. Am. Chem. Soc.* 1992, *114*, 10024-10035.

(4) Potoff, J. J.; Siepmann, J. I. Vapor–Liquid Equilibria of Mixtures Containing Alkanes, Carbon Dioxide, and Nitrogen *AIChE J.* 2001, *47*, 1676-1682.

(5) Bae, Y.-S.; Yazaydın, A. Ö.; Snurr, R. Q. Evaluation of the BET Method for Determining Surface Areas of MOFs and Zeolites That Contain Ultra-Micropores *Langmuir* 2010, *26*, 5475-5483.

(6) Gelb, L. D.; Gubbins, K. E. Pore Size Distributions in Porous Glasses: A Computer Simulation Study *Langmuir* 1998, *15*, 305-308.